JACS
JOURNAL OF THE AMERICAN CHEMICAL SOCIETY

Article

Optical Supramolecular Sensing of Creatinine

Andrés F. Sierra, Daniel Hernández-Alonso, Miguel Angel Romero, Jose Antonio Gonzalez Delgado, Uwe Pischel, and Pablo Ballester

J. Am. Chem. Soc., **Just Accepted Manuscript** • DOI: 10.1021/jacs.9b12071 • Publication Date (Web): 11 Feb 2020

Just Accepted

is published by the American Chemical Society. 1155 Sixteenth Street N.W., Washington, DC 20036

Optical Supramolecular Sensing of Creatinine.

Andrés F. Sierra[1,4], Daniel Hernández-Alonso[1], Miguel A. Romero[2], José A. González-Delgado[2], Uwe Pischel[2,*] and Pablo Ballester[1,3,*].

[1]Institute of Chemical Research of Catalonia (ICIQ), The Barcelona Institute of Science and Technology, Avgda. Països Catalans 16, 43007 Tarragona (Spain).

[2]CIQSO - Center for Research in Sustainable Chemistry and Department of Chemistry, University of Huelva, Campus de El Carmen s/n, E-21071 Huelva (Spain).

[3]Catalan Institution of Research and Advanced Studies (ICREA), Passeig Lluís Companys 23, 08018 Barcelona (Spain).

[4]Universitat Rovira i Virgili, Departament de Química Analítica i Química Orgànica, c/Marcel·lí Domingo, 1, 43007 Tarragona (Spain).

ABSTRACT: Calix[4]pyrrole phosphonate-cavitands were used as receptors for the design of supramolecular sensors for creatinine and its lipophilic derivative hexylcreatinine. The sensing principle is based on indicator displacement assays of an inherently fluorescent guest dye or a black-hole quencher from the receptor's cavity by means of competition with the creatinine analytes. The systems were thermodynamically and kinetically characterized regarding their 1:1 binding properties by means of nuclear magnetic resonance spectroscopy (^{1}H and ^{31}P NMR), isothermal titration calorimetry, and optical spectroscopies (UV/vis absorption and fluorescence). For the use of the black-hole indicator dye, the calix[4]pyrrole was modified with a dansyl chromophore as signaling unit that engages in Förster resonance energy transfer with the indicator dye. The 1:1 binding constants of the indicator dyes are in the range of 10^{7} M^{-1}, while hexylcreatinine showed values around (2-4) × 10^{5} M^{-1}. The competitive displacement of the indicators by hexylcreatinine produced supramolecular fluorescence turn-on sensors that work at micromolar analyte concentrations that are compatible with those observed for healthy as well as sick patients. The limit of detection for one of the systems reached submicromolar ranges (110 nM).

INTRODUCTION

The level of creatinine (**Cr**, see Figure 1) in human bodily fluids is a widely applied clinical indicator for monitoring kidney and renal functions.[1,2] Creatinine is a metabolic waste product, being related to muscle activity, and any anomalous secretion due to organ malfunction leads inevitably to higher concentrations of **Cr** in blood serum and/or urine. Methods for molecular biosensing of creatinine using simple fluorescent probes or in combination with bioconjugates have been reported.[2,3,4,5,6] While these latter approaches rely on unspecific interactions between creatinine and the probe molecule, supramolecular sensing offers distinct benefits for the design of selective and specific sensors by building on size, shape and function complementarity between receptor and analyte. Unfortunately, most synthetic receptors designed for creatinine binding are flat and edge-functionalized with divergent hydrogen bonding motifs.[7,8,9,10,11] These characteristics make them a non-ideal choice for supramolecular sensing design. Hence, it is not surprising that supramolecular approaches to creatinine sensing, using synthetic receptors, are very scarce in literature.[12,13]

The selection of the synthetic receptor unit is a key element in the design of supramolecular sensors. In this respect, aryl-extended calix[4]pyrroles[14] and their cavitand derivatives are well-known receptors for the effective binding of neutral polar species, as well as mono- and poly-atomic anions.[15] The superior binding properties of these receptors are inherent to the structural elements that relate to their cone conformation. Moreover, aryl-extended calix[4]pyrroles can be synthetically elaborated both at their upper and lower rims. These structural modifications of the receptor scaffold are translated into modulations of solubility and binding properties. Fluorescent calix[4]pyrrole chemosensors for the recognition of anions[16,17,18,19,20,21,22,23,24,25] and cations[26,27] are known in the literature. In contrast, the development of fluorescent calix[4]pyrrole chemosensors for the detection and quantification of relevant polar biomolecules remains practically unexplored.[28]

In 2016, we introduced an ion-selective-electrode (ISE) suitable for the detection of **Cr** in bodily fluids.[29] This ISE hinged on the use of a novel mono-phosphonate calix[4]pyrrole **1** as ionophore (Figure 1). Receptor **1** displayed high affinity for **Cr** and its protonated form **Cr**•H^{+}. In contrast to the previously published plane creatinine receptors,[7,10,11,12] macrocycle **1** features a deep aromatic cavity that is functionalized with a single phosphonate group at the open end (upper rim) and four pyrrole NHs at the closed end.

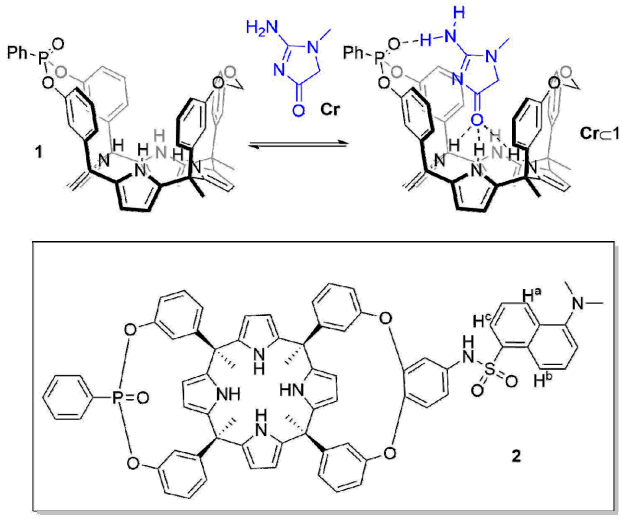

Figure 1. Top: molecular structures of receptor **1**, creatinine **Cr**, the 1:1 inclusion complex **Cr⊂1** and its binding equilibrium. Bottom: structure of the dansyl-modified calix[4]pyrrole receptor **2.**

The cavity dimensions of **1** are ideal for the inclusion of **Cr** by surrounding most of its surface. The polar groups of **1** offer complementary hydrogen-bonding, π-π, CH-π interactions with the included **Cr**. These attributes translate into an efficient binding for **Cr** in organic solvents. Moreover, the 1:1 **Cr⊂1** inclusion complex is kinetically stable on the ^{1}H NMR chemical shift timescale.

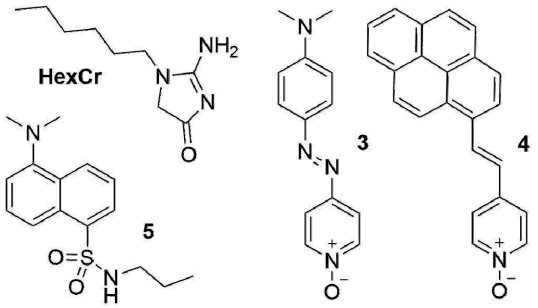

Figure 2. Molecular structures of **HexCr**, the *para*-substituted pyridyl-*N*-oxides **3** and **4** and the dansyl reference model **5.**

Drawing on calix[4]pyrrole **1** we present herein optical supramolecular sensors for creatinine and derivatives. In an expansion, the scaffold of **1** was modified with a dansyl fluorophore, yielding receptor **2** (Figure 1). Using fluorescence emission as output signal of a molecular sensor provides a convenient way of analyte detection, even with the naked eye. In addition, fluorescence can be monitored for relatively low concentrations (sub-micromolar) of the sensor, improving the sensitivity further.

A priori two photophysical design strategies (see Scheme 1) based on the popular and functionally flexible competitive indicator-displacement-assays (IDA),[30,31] could be followed with receptors **1** and **2**.

Scheme 1. Schematic approaches to optical supramolecular sensing of creatinine (analyte) using a calix[4]pyrrole scaffold (receptor). Top: Displacement of a black-hole quencher (BHQ) and deactivation of FRET quenching of a receptor-appended fluorophore (signaling unit). Bottom: Displacement of a fluorescent dye.

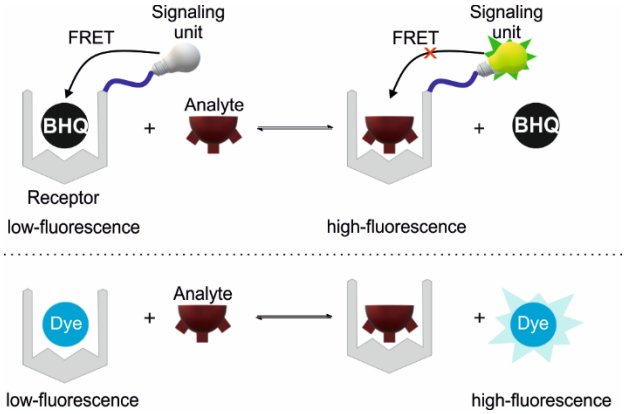

In both cases, we choose pyridyl-*N*-oxides as binding motifs of the indicator guest. Pyridyl-*N*-oxides are known to form host-guest complexes with calix[4]pyrroles having binding constants (10^{6}-10^{7} M^{-1})[32] that are comparable with or slightly higher than those of **Cr** and its derivatives. On the one hand, receptor **2** could be combined with a black-hole quencher guest (**3**, Figure 2) which on binding deactivates the dansyl fluorescence by Förster resonance energy transfer (FRET). The competitive displacement of the indicator by **HexCr** (as lipophilic **Cr** analogue) is expected to be signaled by the observation of fluorescence turn-on. On the other hand, receptor **1** could be combined with a fluorescent guest (**4**, Figure 2). On binding by the receptor, the guest would then undergo fluorescence quenching which is inverted on competitive displacement with **HexCr**. This again yields a fluorescent turn-on sensor. Based on these approaches highly sensitive optical supramolecular sensors for creatinine derivatives are presented.

RESULTS AND DISCUSSION

Synthesis

The synthesis of receptor **2** involved four reaction steps starting from the known α,α,α,α-tetra-hydroxy-calix[4]pyrrole **6** (Scheme 2).[33] The nitro mono-aryl bridged intermediate **7** was prepared using reaction conditions previously reported for a structurally related compound.[34] The nitro-diol-cavitand **7** was isolated, as a racemic mixture, after column chromatography purification in 32 % yield. The incorporation of the bridging phosphonate group was achieved by reacting the nitro-diol **7** with phenylphosphonic dichloride using triethylamine as base. The reaction produced a mixture of two diastereoisomers, **8in** and **8out**, which differ in the relative spatial orientation of the P=O group with respect to the aromatic cavity. Diasteroisomers **8in** and **8out** were isolated as pure compounds after column chromatography purification of the reaction crude in 46% and 22% yield, respectively.

Scheme 2. Synthetic scheme for the preparation of the fluorescent mono-phosphonate cavitand 2. The structures of the cavitands 7 and 8in are depicted as single enantiomers for simplicity.

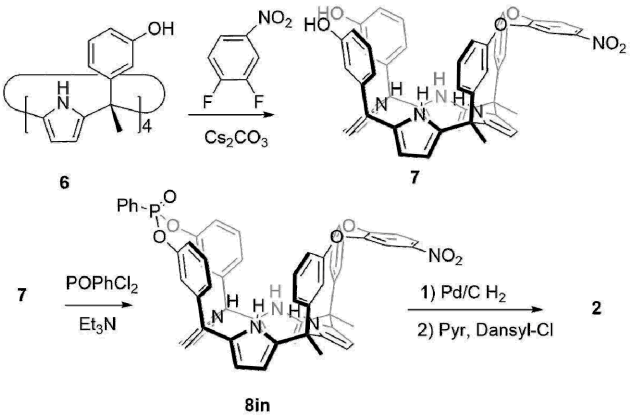

Gratifyingly, single crystals of **8in** and **8out** (Figures S63 and S64), that were suitable for X-ray diffraction analysis, were obtained from acetone and dichloromethane solutions, respectively (Figure 3). In the solid state, **8in** showed the aryl-extended calix[4]pyrrole core in cone conformation with one molecule of acetone included in the aromatic cavity. The four pyrrole NHs interact with the acetone guest via hydrogen bonding. The nitro-aryl bridging group adopted a pseudo-equatorial conformation.[35]

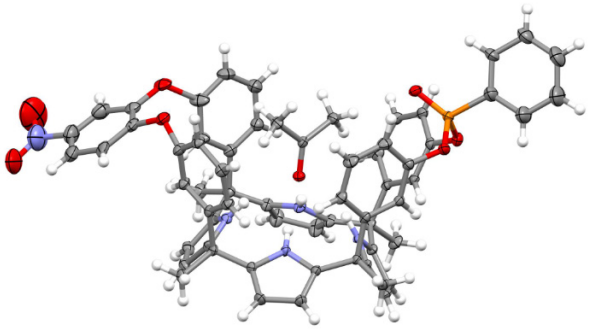

Figure 3. X-ray structure of the CH_3COCH_3⊂**8in** inclusion complex, thermal ellipsoids for C, N, O and P atoms set at 50% probability; H atoms are shown as spheres of 0.20 Å diameter.

The catalytic hydrogenation of the nitro-compound **8in**, using 10% Pd/C, yielded quantitatively the corresponding amino-derivative, which was used without further purification in the coupling reaction with dansyl chloride. The fluorescent dansyl amide mono-phosphonate cavitand receptor **2** was obtained in 98% yield as a racemic mixture. All attempts to separate the enantiomers of **2**, using chiral HPLC, were unsuccessful. However, because creatinine is non-chiral, no difference for the sensing is expected for the two stereoisomers. Receptor **2** was characterized by a full set of high-resolution spectra (Figures S9 to S18).

In turn, the precursor of the pyridyl-*N*-oxide dye **4** was prepared following a reported procedure.[36] The *N*-oxidation reaction of the synthesized pyridine was performed using *m*-chloroperoxybenzoic acid (*m*-CPBA).[37]

The fluorescent *N*-oxide **4** was isolated after column chromatography purification, using neutral alumina, in 58% yield. This strategy was not implemented in the synthesis of **3** owing to the presence of additional nitrogen atoms susceptible to *N*-oxidation with the peroxyacid treatment.[38] Instead, we synthesized **3** following a reported procedure that involves the preparation of 4-amino-pyridine-*N*-oxide, its diazotization and subsequent coupling with dimethyl-aniline.[39] Starting from 4-Boc-amino-pyridine, we isolated **3** in high purity and 11% overall yield.

Finally, due to the reduced solubility of **Cr** in organic solvents, we prepared the lipophilic derivative **HexCr**. The compound was obtained, following a known protocol, [40] by treating methyl *N*-cyano-*N*-hexyl-aminoacetate with aqueous ammonia at room temperature. **HexCr** proved to be soluble up to 1.5 mM in dichloromethane and chloroform, thereby enabling binding studies by NMR spectroscopy (see below).

Binding studies of 2 with HexCr

We initially probed the interaction of **2** with **HexCr** using ^{1}H and ^{31}P NMR spectroscopy. The ^{1}H NMR spectrum of **2** at mM concentration in $CDCl_3$ solution showed sharp and well-resolved proton signals (Figure 4a, left panel).

The addition of 0.5 equiv. of **HexCr** to a mM solution of **2** in $CDCl_3$ produced the appearance of a new set of signals that were assigned to the protons of the bound host (Figure 4b, left panel). Remarkably, the bound pyrrole NHs resonated as four sharp singlets around 9.8 ppm. The significant downfield shift ($\Delta\delta$ = +1.5-1.7 ppm) experienced by the NH protons testifies their involvement in hydrogen bonding interactions with the oxygen atom of the bound **HexCr**. Moreover, we detected two new signals in the aliphatic region of the spectrum. These signals were assigned to the protons H^1 and H^7 of the bound **HexCr**. The H^1 proton experienced a large upfield shift ($\Delta\delta$ = –2.71 ppm) with respect to its chemical shift value in the free **HexCr** (Figure S47). This observation supports the deep inclusion of **HexCr** in the aromatic cavity of **2**, where the H^1 proton experiences the shielding effect exerted by the four *meso*-phenyl groups of the receptor.

The addition of incremental amounts of **HexCr** produced a gradual increase in intensity of the proton signals assigned to bound **2** at the expenses of those of the free counterpart. In the presence of 1 equiv of **HexCr**, only the proton signals corresponding to the bound host **2** were observable (Figure S47). Finally, an excess of **HexCr** produced the appearance of the proton signals corresponding to free guest (Figure 4c, left panel).

An analogous behavior was observed in the acquired ^{31}P NMR spectra of the solutions. The ^{31}P NMR spectrum of **9in** showed a somewhat broadened singlet resonating at 15.5 ppm corresponding to the phosphorous atom of the inwardly directed P=O group (Figure 4a right panel). In the presence of incremental amounts of **HexCr**, the intensity of this phosphorous signal decreased and a new sharp singlet, resonating at 13.7 ppm, was observed. In the presence of 1.5 equiv of **HexCr,** only the phosphorus signal assigned to the P=O group in bound **2** was detected (Figure 4c right panel).

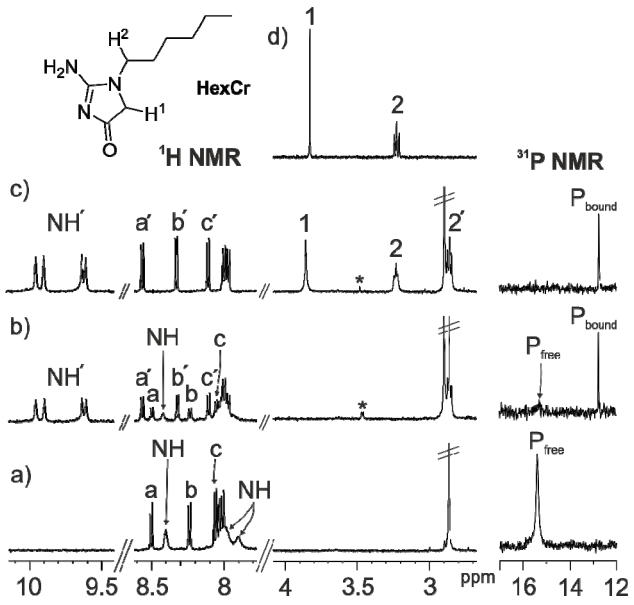

Figure 4. Left panel, selected regions of the ^{1}H NMR spectra (500 MHz, 298 K) of $CDCl_3$ solutions containing fluorescent receptor 2 and **HexCr** in different molar ratios: a) Free **2**; b) **2** + 0.5 equiv.; c) **2** + 1.5 equiv.; d). Trace shows one region of the ^{1}H NMR spectrum of **HexCr**. Right panel, corresponding ^{31}P NMR spectra (202 MHz, $CDCl_3$, 298 K). Primed letters and numbers correspond to the proton signals in the **HexCr⊂2** complex. Proton assignment of **HexCr** is shown in the inset structure. For the proton assignment of **2** see Figure 1. * Residual methanol peak. See supporting information for a more detailed preparation of the analyzed solution mixtures.

In summary, these results indicate that receptor **2** and **HexCr** exclusively formed a 1:1 inclusion complex, **HexCr⊂2**. In this complex, the **HexCr** is deeply immersed in the aromatic cavity of the calix[4]pyrrole **2** in its cone conformation. The binding process displayed slow chemical exchange dynamics in the ^{1}H and ^{31}P NMR chemical shift timescales between free and bound counterparts.

The kinetic stability of the complex was accompanied by a high thermodynamic stability. Thus, the exclusive observation of the signals of the bound host **2** in the ^{1}H and ^{31}P NMR spectra acquired in the presence of 1 equiv of **HexCr**, allowed us to estimate that the stability constant of the **HexCr⊂2** complex should be larger than 10^4 M^{-1}.

The **HexCr⊂2** complex was fully characterized using 2D NMR experiments (COSY, ROESY Figure S48 to S51)**.** To gain additional insight into the three-dimensional structure of the **HexCr⊂2** complex, the putative 1:1 inclusion was energy minimized (according to frequency calculation) at the BP86[41,42]-D3[43,44]/def2-SVP[45] level of theory using a polarizable continuum solvent model (PCM) for chloroform as implemented in Gaussian 09.[46] In analogy to the previously described mono-phosphonate methylene-bridged receptor **1**, the energy-minimized structure of the **HexCr⊂2** complex showed that the aromatic cavity of **2** nicely complements in terms of size, shape and functionalization the included **HexCr** (Figure 5). The average distance between the centroids of **HexCr** and the dansyl group is in the range of 12 Å.

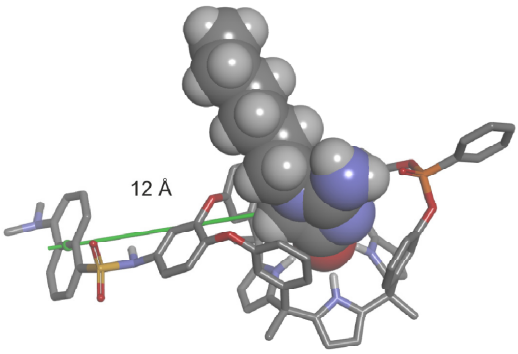

Figure 5. Energy-minimized structure of the **HexCr⊂2** complex (PB86-D3/def2-SVP, CPM/chloroform). The non-polar hydrogen atoms of receptor **2** were removed for the sake of clarity. The encapsulated **HexCr** molecule is shown as CPK model.

In order to assess the accurate value of the stability constant of the **HexCr⊂2** complex, we performed isothermal titration calorimetry (ITC) experiments. The successive addition of aliquots of a chloroform solution of receptor **2** (2.2 mM) to a solution of **HexCr** (0.3 mM) in the same solvent produced a gradual release of heat corresponding to the binding event (Figure 6, top). The normalized integrated heats were corrected for dilution effects. This provided a sigmoidal binding isotherm with an inflection point close to a host: guest ratio of 1 (Figure 6, bottom), as expected for 1:1 binding.

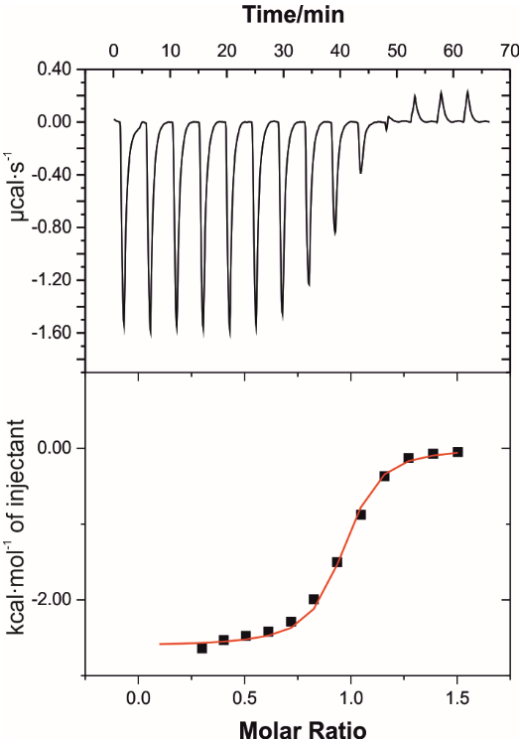

Figure 6. Raw data (heat vs. time) for the calorimetry titration of **HexCr** (0.3 mM) with **2** (2.2 mM) performed at 288 K (top). Fit of the integrated and corrected calorimetric data to the one-site binding model (bottom). Note that the first two points were excluded from the fitting.

The fit of the calorimetric titration data to a 1:1 binding model returned an accurate value of the binding constant as K_a(**HexCr⊂2**) = (4.5 ± 0.4) × 10^5 M^{-1}. In addition, the fit also provided the binding enthalpy ΔH = −10.9 ± 0.4 kJ·mol^{-1}, which allowed us to calculate $T\Delta S$ as 20.2 ± 0.6 kJ·mol^{-1} (298 K). These results indicate that the binding of **HexCr** by receptor **2** is mainly entropically driven. In accordance with previous interpretations, the de-solvation of the binding partners and the solvation of the formed inclusion complex are thought to play an important role in the complexation process of aryl-extended calix[4]pyrrole cavitand receptors.[47]

Interaction of receptor 2 with dye 3 probed by fluorescence spectroscopy and ITC experiments

The absorption spectrum of **2** in chloroform (blue line in Figure 7) shows an intense band with a maximum at 347 nm (ε = 4300 M^{-1}·cm^{-1}), typical for the dansyl chromophore (compare with model **5**; $\lambda_{abs,max}$ = 341 nm, ε = 4400 M^{-1}·cm^{-1}). Further, an intense absorption band with a maximum at 249 nm, which is characteristic for the π,π*-transitions of the aryl-extended calix[4]pyrrole, is present (see Figure S37). Excitation at 347 nm produces the characteristic and intense fluorescence emission of an intramolecular charge-transfer (ICT) excited state with a maximum at $\lambda_{fluo,max}$ = 509 nm (green line in Figure 7). The fluorescence quantum yield of **2** was determined as Φ_{fluo} = 0.45 and the lifetime measured as τ_{fluo} = 14.8 ns. These data compare absolutely to the photophysical characteristics of the dansyl model compound **5** ($\lambda_{fluo,max}$ = 495 nm, Φ_{fluo} = 0.46, τ_{fluo} = 13.3 ns) in the same solvent. Thus, it was concluded that the calix[4]pyrrole has no significant quenching effect on the appended fluorophore.

For the realization of the IDA with the reporter pair **3⊂2** we characterized the complexation of the pyridyl-*N*-oxide **3**, an analogue of the well-known 4-((4-(dimethylamino)phenyl)azo)benzoic acid (DABCYL). DABCYL is a very popular black-hole quencher in FRET-based quenching pairs for nucleic acids and proteins.[48,49] Dye **3** is an efficient light absorber between 400 nm and 550 nm ($\lambda_{abs,max}$ = 480 nm, ε = 39500 M^{-1}·cm^{-1}); see Figure 7.

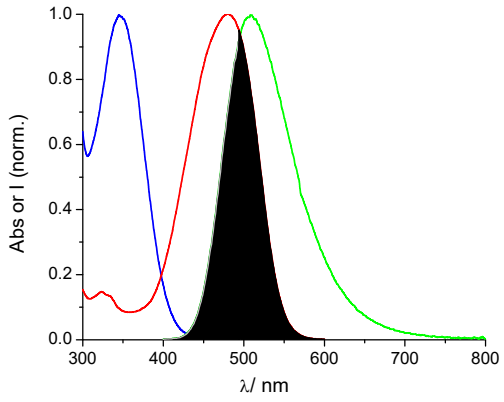

Figure 7. UV/vis-absorption spectra of **2** (blue) and **3** (red) and the fluorescence spectrum of **2** (green). In black the spectral of overlap is illustrated.

This results in a significant spectral overlap with the dansyl emission (J = 1.2 × 10^{-10} cm^6·mol^{-1}), which translates into a critical FRET radius of R_0 = 43.7 Å. Taking into account the modeled distance (~ 13 Å, Figure S66) between the dansyl energy donor and **3** as the acceptor dye in the **3⊂2** complex, a quantitative FRET process should result (Φ_{FRET} ca. 1). Hence, we expected that on complexation of **3** by **2** ([2] = 5 μM) the fluorescence of the dansyl chromophore was efficiently quenched. Indeed, the fluorescence quenching was practically quantitative (ca. 95%) when 2 equiv of **3** is added. The fluorescence titration curve was fitted according to a 1:1 binding model yielding a binding constant of K_a(**3⊂2**) = (1.2 ± 0.5) × 10^7 M^{-1} (corrected for minor inner-filter effects due to the addition of a chromophoric titrator); see Figure 8.

An independent fluorescence lifetime quenching experiment indicated that the quenching was not of dynamic nature (an invariable lifetime of 14.8-14.9 ns was measured in the absence and presence of **3** as quencher). Hence, intermolecular quenching can be ruled out in the investigated concentration range.

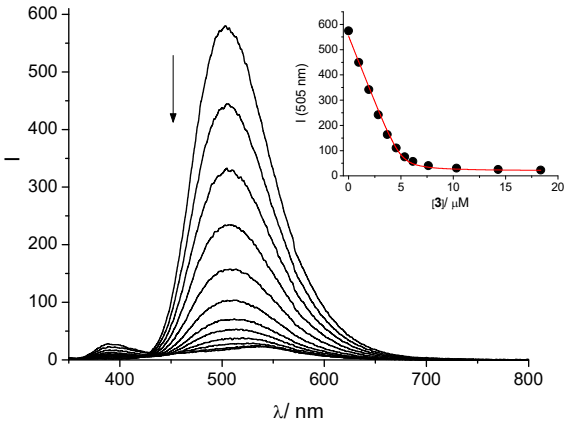

Figure 8. Emission spectra of **2** (5 μM) registered on addition of increasing amounts of **3** in chloroform; λ_{exc} = 317 nm. Inset: Plot of the emission change at 505 nm (black circles) vs concentration of **3**. The red line corresponds to the fit of the titration data to a binding model that considers the formation of the 1:1 complex, **3⊂2**.

Next, we probed the interaction of **3** with receptor **2** by means of ITC experiments (see Figure S59). The titrations produced rectangular binding isotherms with the height corresponding exactly to ΔH and the sharp-increase occurring at the stoichiometric equivalence point: host:guest ratio of 1. This is the expected result for very tight binding and resulted only useful to estimate that K_a(**3⊂2**) was larger than 10^7 M^{-1}. The estimated magnitude of the binding constant value is in complete agreement with the value calculated from the fluorescence titrations. While the enthalpic contribution to binding, ΔH, could be accurately determined as −34.7 kJ·mol^{-1} from the height of the isotherm, the corresponding entropic term, which should be positive, could not be derived owing to the estimative nature of K_a(**3⊂2**). An accurate determination of K_a(**3⊂2**) using ITC experiments required working in more dilute conditions, that is reducing the "*c*" value. This approach was not

experimentally feasible owing to reduced heat release of the binding process, which dropped below the instrument's sensitivity (3-5 µcal per injection) at lower concentrations.[50]

Competitive IDA of the 3⊂2 ensemble with HexCr

We prepared an equimolar mixture of **3** and **2** (1 µM) in chloroform solution. At this concentration complex formation is reached to an extent of 83%. The solution was titrated with incremental amounts of **HexCr**.[51] According to the expectations, on displacement of **3**, as quencher of the dansyl fluorescence, a turn-on effect was observed. For the addition of ca. 70 equiv **HexCr** a 4-fold fluorescence enhancement at 505 nm was registered; see Figure 9. Noteworthy, **HexCr** does not exercise any significant quenching effect on the dansyl fluorophore when included in the cavity of receptor **2** (Figure S37).

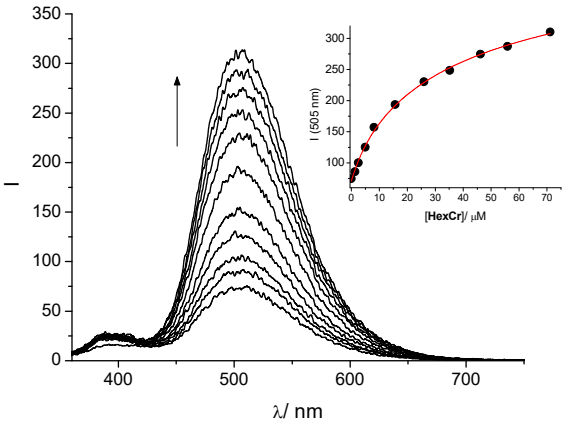

Figure 9. Emission spectra registered during the competitive IDA of the **3⊂2** ensemble with **HexCr**; λ_{exc} = 317 nm. The initial fluorescence is due to the minor fraction (17%) of free **2** at the used equimolar concentration (1 µM). Inset: Plot of the changes in emission at 505 nm vs concentration of **HexCr**. The red line corresponds to the fit of the titration data to a competitive binding model that considers the formation of the **3⊂2** and **HexCr⊂2** complexes.

Hence, the observed fluorescence enhancement corresponds to the undisturbed response of the IDA. The fit of the competitive titration data to a competitive binding model of two 1:1 complexes returned a stability constant for the **HexCr⊂2** complex of K_a(**HexCr⊂2**) = (3.2 ± 0.4) × 10^5 M^{-1}. This value is in excellent agreement with the one obtained in the ITC experiment; (4.5 ± 0.4) × 10^5 M^{-1} (see above).

The need for a large excess **HexCr** is explained by the difference in the binding constant values of the competitors; see above. Gratifyingly, the concentration range that is required to obtain a visible fluorescence response of the **3⊂2** IDA coincides with or is well below the expected clinical levels of creatinine in blood serum (60-420 µM) or urine (3-25 mM) for healthy individuals.[2] In the case of kidney or renal dysfunction these values are dramatically increased. We determined the limit of detection (LOD) of the **3⊂2** IDA to be ca. 110 nM.

Noteworthily, very similar results were obtained when creatinine (**Cr**) was used instead of the lipophilic version **HexCr** (Figure S42). On addition of **Cr** to the ensemble **3⊂2** (both components at 1 µM) the fluorescence of the system increased significantly (factor of 2.7 for 50 µM **Cr**). The limited solubility of **Cr** in chloroform (≤ 50 µM) precluded the registration of a complete titration curve. However, based on the obtained data, it can be safely stated that a lower limit for the binding constant of the **Cr⊂2** complex is ca. 5 × 10^4 M^{-1}. Hence, in terms of its sensitivity range the herein developed fluorescent IDA is fully compatible with **Cr**. The **Cr⊂2** complex was fully characterized by means of 1D and 2D high-resolution NMR experiments (Figures S52-S54).

Finally, we tested the possible interference of other biologically relevant analytes. For this purpose, urea and *L*-proline, as an abundant amino acid, were chosen. The separate addition of these compounds to the ensemble **3⊂2** (both components at 1 µM) yielded fluorescence increase factors of 1.4 (*L*-proline) and 2.6 (urea); see Figures S38 and S39. These responses are significant, however, smaller than those observed for **HexCr** (see above).

Development of an IDA based on the non-fluorescent receptor 1

The previously described receptor **1**, which is known to be an excellent host for **Cr**, is non-fluorescent.[29] However, by introducing a fluorescent guest, receptor **1** can be integrated in an optical IDA suitable for **HexCr** sensing. For this purpose, we designed the guest dye **4**, containing the pyridyl-*N*-oxide binding motif connected to a pyrene chromophore by an ethenyl spacer. Dye **4** features an absorption maximum at 394 nm (ε = 32600 $M^{-1}\cdot cm^{-1}$) and fluoresces with maximum at 474 nm (Φ_{fluo} = 0.21, τ_{fluo} = 1.11 ns). The rather broad emission band and relatively large Stokes shift underpin the ICT character of the fluorescent state.

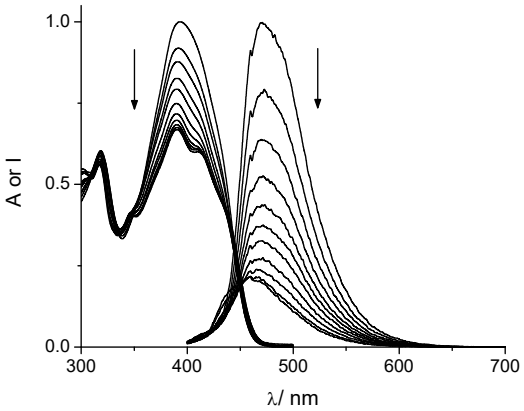

Figure 10. UV/vis absorption (left) and fluorescence emission (right) spectra of **4** on addition of receptor **1**. The fluorescence spectra were obtained for excitation at 350 nm.

The UV/vis absorption titration of **4** with incremental amounts of receptor **1** (inverse titration) provided a set of spectra displaying one quasi-isosbestic point at 350 nm (see Figure 10). This is the expected result for the exclusive formation of a 1:1 complex in binding systems involving only two absorbing species: the unbound dye **4** and its inclusion complex **4⊂1**.[52] The titration was also monitored by fluorescence spectroscopy; see Figure 10. In the course of the titration the fluores-

cence was significantly quenched (ca. 80% on addition of 2.5 equiv **1**) and at the endpoint a slightly blue-shifted emission spectrum ($\Delta\lambda$ = -11 nm) was observed. This the likely result of the disturbance of the ICT state on interaction pyridine-*N*-oxide moiety with the host, leading to the observed quenching. The analysis of the emission changes of the dye *vs* the concentration of **1**, using a 1:1 binding model, provided the binding constant value for the corresponding inclusion complex; K_a(**4**⊂**1**) = (1.2 ± 0.2) × 10^7 M^{-1} (Figure S40). ITC experiments (Figure S61) confirmed the tight and strong 1:1 binding with an exothermic enthalpic contribution of ΔH = –38.0 ± 0.4 kJ·mol^{-1}. However, for the same reasons as discussed above for the binding of **3** by host **2**, only a lower limit of 10^7 M^{-1} can be stated for the binding constant value. Noteworthily, this agrees nicely with the more accurate data obtained by fluorescence titration.

Finally, we tested the ensemble **4**⊂**1** in a competitive IDA with **HexCr**.[53] The sensing ensemble consisted of equimolar amounts (each 1 μM) of receptor **1** and indicator **4**, assuring a complexation degree of 80%. The incremental addition of **HexCr** restored the emission of the dye (fluorescence enhancement factor of 2.3 at 50 μM **HexCr**). The corresponding titration curve was analyzed using a binding model of two competitive complexes. The fit provided a binding constant of (4.3 ± 0.5) × 10^5 M^{-1} for the **HexCr**⊂**1** complex. This value is again in good agreement with the one determined in ITC experiments; K_a(**HexCr**⊂**1**) = (1.5 ± 0.3) × 10^5 M^{-1}(Figure S60). The ITC experiment provided further information on the enthalpic and entropic contributions to binding: ΔH = –7.8 ± 0.1 kJ·mol^{-1} and $T\Delta S$ as -19.8 ± 0.1 kJ·mol^{-1} (298 K). This led to the conclusion that the binding of **HexCr** by **1** is mainly entropically driven.

Not surprisingly, the IDA with **Cr** yielded practically the same switch-on response as for **HexCr** (Figure S43). On addition of 50 μM **Cr** a fluorescence enhancement factor of 1.8 was obtained. The fitting of the competitive binding titration returned a binding constant of K_a(**Cr**⊂**1**) = (3.0 ± 1.0) × 10^5 M^{-1}.

Future challenges and developments

The future challenges of the described supramolecular design include the improvement of their sensing selectivity and the compatibility with aqueous media. On the one hand, as herein demonstrated the current design shows interferences with other biologically relevant analytes, such as proline and urea. In practical terms, this limitation could be avoided by previous extractive separation of creatinine. On the other hand, the issue of water solubility of the calix[4]pyrrole receptor and/or the dyes can be addressed by synthetic modifications involving the incorporation of ionizable and charged groups in their scaffolds periphery. However, it is expected that the binding constant of creatinine with the water-soluble versions of the receptor would drop considerably owing to the polar nature of the analyte and the competition of water for hydrogen bonding. This drawback might be partially overcome by performing the sensing experiments in microheterogeneous media, such as micelles and liposomes. We are currently expanding our efforts in these directions and we expect to report our findings in due course.

CONCLUSIONS

Calix[4]pyrrole-derived IDAs were designed to enable the efficient sensing of **Cr** and its derivative **HexCr**. The calix[4]pyrrole receptors, **1** and **2**, operates according to the principles of size, shape and functional complementarity. **Cr** and derivatives are included in the receptor's cavities (K_a ca. 4.5 × 10^5 M^{-1}), establishing five complementary hydrogen bonds: four with pyrrole NHs and one with the upper rim phosphonate group. In one version of the developed sensors, compound **2**, the receptor unit features a covalently attached dansyl fluorophore. This provides a means for FRET-based IDA through the displacement of a black-hole quencher **3** by **Cr** or its lipophilic analogue **HexCr**. In another version, the inherently fluorescent pyrene-based dye **4** formed a reporter pair with receptor **1**. In both developed IDAs, the indicator dyes interact with the calix[4]pyrrole cavitand scaffolds through complexation of the pyridyl-*N*-oxide motif (K_a ca. 10^7 M^{-1}). The two developed IDAs work in organic chlorinated solvents at a range of concentrations that coincide with those in which **Cr** is present in bodily fluids (blood serum and urine). Remarkably, the **3**⊂**2** IDA features a limit of detection as low as 110 nM, drawing on the high sensitivity of the fluorescence measurements and the significant affinity of receptor **2** for **HexCr** and **Cr**. The developed IDAs rely on a combination of hydrogen bonding, π-π and CH-π interactions, as driven forces of the molecular recognition events. To the best of our knowledge, the reported work describes unprecedented examples of fluorescent supramolecular sensors for creatinine.

ASSOCIATED CONTENT

Supporting Information

Experimental procedures and characterization data of the synthesized compounds, NMR, UV/vis and emission spectra of the binding studies. X-ray crystals structures (CIF files) of **HexCr**, **7**, **8in** and **8out**. Fits of the fluorescent titration data. Figures of the raw data and normalized heats obtained in the isothermal titration calorimetry (ITC) experiments. This material is available free of charge via the Internet at http://pubs.acs.org.

The Supporting Information is available free of charge on the ACS Publications website.

AUTHOR INFORMATION

Corresponding Author

* E-mail: pballester@iciq.es; uwe.pischel@diq.uhu.es

ACKNOWLEDGMENT

This work was supported by Gobierno de España MINECO and FEDER funds (CTQ2017-84319-P for P.B. and CTQ2017-89832-P for U.P.), CERCA programme/Generalitat de Catalunya, and AGAUR (2017-SGR-1123). We also thank Dr Eduardo C. Escudero-Adán, X-ray Diffraction Unit of ICIQ, for help with the analysis of the X-ray crystallographic data and Dr Luis Martínez-Crespo for experimental assistance and helpful discussions in the initial phases of the project.

REFERENCES

[1] Wyss, M.; Kaddurah-Daouk, R. Creatine and Creatinine Metabolism. *Physiol. Rev.* **2000**, *80*, 1107-1213.

[2] Cánovas, R.; Cuartero, M.; Crespo, G. A. Modern creatinine (Bio)sensing: Challenges of point-of-care platforms. *Biosensors and Bioelectronics* **2019**, *130*, 110-124.

[3] Pal, S.; Lohar, S.; Mukherjee, M.; Chattopadhyay, P.; Dhara, K. A fluorescent probe for the selective detection of creatinine in aqueous buffer applicable to human blood serum. *Chem. Commun. (Cambridge, U. K.)* **2016**, *52*, 13706-13709.

[4] Rajamanikandan, R.; Ilanchelian, M. Protein-protected red emittive copper nanoclusters as a fluorometric probe for highly sensitive biosensing of creatinine. *Anal. Methods* **2018**, *10*, 3666-3674.

[5] Ellairaja, S.; Shenbagavalli, K.; Vasantha, V. S. Ultrasensitive Fluorescent Biosensor for Creatinine Determination in Human Biofluids Based on Water Soluble Rhodamine B Dye-Au3+ ions Conjugate. *ChemistrySelect* **2017**, *2*, 1025-1031.

[6] Chen, T.; Xie, N.; Viglianti, L.; Zhou, Y.; Tan, H.; Tang, B. Z.; Tang, Y. Quantitative urinalysis using aggregation-induced emission bioprobes for monitoring chronic kidney disease. *Faraday Discuss.* **2017**, *196*, 351-362.

[7] Beckles, D. L.; Maioriello, J.; Santora, V. J.; Bell, T. W.; Chapoteau, E.; Czech, B. P.; Kumar, A. Complexation of Creatinine by Synthetic Receptors. *Tetrahedron* **1995**, *51*, 363-376.

[8] Bell, T. W.; Hext, N. M.; Khasanov, A. B. Binding biomolecules with designed, hydrogen-bonding receptors. *Pure Appl. Chem.* **1998**, *70*, 2371-2377.

[9] Bell, T.; Firestone, A.; Liu, J.; Ludwig, R.; Rothenberger, S. In *Inclusion Phenomena and Molecular Recognition*; Atwood, J., Ed.; Springer US: 1990, p 49-56.

[10] Bühlmann, P.; Badertscher, M.; Simon, W. Molecular Recognition of Creatinine. *Tetrahedron* **1993**, *49*, 595-598.

[11] Bühlmann, P.; Simon, W. Neutral Hosts for the Complexation of Creatinine. *Tetrahedron* **1993**, *49*, 7627-7636.

[12] Bell, T. W.; Hou, Z.; Luo, Y.; Drew, M. G. B.; Chapoteau, E.; Czech, B. P.; Kumar, A. Detection of Creatinine by a Designed Receptor. *Science* **1995**, *269*, 671-674.

[13] Mei, M. H.; Wu, S. K. A fluorescent chemosensor for recognition of creatinine. *Acta Chim. Sin.* **2002**, *60*, 866-869.

[14] Gale, P. A.; Sessler, J. L.; Král, V.; Lynch, V. Calix[4]pyrroles: Old Yet New Anion-Binding Agents. *J. Am. Chem. Soc.* **1996**, *118*, 5140-5141.

[15] Kim, D. S.; Sessler, J. L. Calix[4]pyrroles: versatile molecular containers with ion transport, recognition, and molecular switching functions. *Chem. Soc. Rev.* **2015**, *44*, 532-546.

[16] Samanta, R.; Kumar, B. S.; Panda, P. K. Calix[4]pyrroles with Shortest Possible Strap: Exclusively Selective toward Fluoride Ion. *Org. Lett.* **2015**, *17*, 4140-4143.

[17] Saha, I.; Lee, J. H.; Hwang, H.; Kim, T. S.; Lee, C.-H. Remarkably selective, non-linear allosteric regulation of anion binding by a tetracationic calix[4]pyrrole homodimer. *Chem. Commun. (Cambridge, U. K.)* **2015**, *51*, 5679-5682.

[18] Taner, B.; Kursunlu, A. N.; Güler, E. The example of calix[4]pyrrole derivative containing Bodipy unit: Fluorometric and colorimetric sensor for F− ion. *Spectrochim. Acta, Part A* **2014**, *118*, 903-907.

[19] Kim, S. K.; Lee, H. G.; Vargas-Zúñiga, G. I.; Oh, J. H.; Lynch, V. M.; Lee, M. H.; Sessler, J. L. A fluorogenic calix[4]pyrrole with a small rigid strap showing different fluorescent responses to anions. *Supramol. Chem.* **2017**, *29*, 651-657.

[20] Ghorpade, T. K.; Patri, M.; Mishra, S. P. Highly sensitive colorimetric and fluorometric anion sensors based on mono and di-calix[4]pyrrole substituted diketopyrrolopyrroles. *Sens. Actuators, B* **2016**, *225*, 428-435.

[21] Anzenbacher, P., Jr.; Jursikova, K.; Sessler, J. L. Second Generation Calixpyrrole Anion Sensors. *J. Am. Chem. Soc.* **2000**, *122*, 9350-9351.

[22] Kataev, E. A.; Backmann, N.; Shumilova, T. A.; Rüffer, T.; Lang, H. Calix[4]pyrroles bearing quinolinium moiety for halide sensing in aqueous solution. *Supramol. Chem.* **2016**, *28*, 53-61.

[23] Sokkalingam, P.; Yoo, J.; Hwang, H.; Lee, P. H.; Jung, Y. M.; Lee, C.-H. Salt (LiF) Regulated Fluorescence Switching. *Eur. J. Org. Chem.* **2011**, *2011*, 2911-2915.

[24] Sokkalingam, P.; Kim, D. S.; Hwang, H.; Sessler, J. L.; Lee, C.-H. A dicationic calix[4]pyrrole derivative and its use for the selective recognition and displacement-based sensing of pyrophosphate. *Chem. Sci.* **2012**, *3*, 1819-1824.

[25] Mulugeta, E.; He, Q.; Sareen, D.; Hong, S.-J.; Oh, J. H.; Lynch, V. M.; Sessler, J. L.; Kim, S. K.; Lee, C.-H. Recognition, Sensing, and Trapping of Bicarbonate Anions with a Dicationic meso-Bis(benzimidazolium) Calix[4]pyrrole. *Chem* **2017**, *3*, 1008-1020.

[26] Bhatt, K. D.; Shah, H. D.; Panchal, M. A switch-off fluorescence probe towards Pb(II) and cu(II) ions based on a calix[4]pyrrole bearing amino-quinoline group. *Luminescence* **2017**, *32*, 1398-1404.

[27] Yoo, J.; Jeoung, E.; Lee, C.-H. Fluorophore-appended calix[4]pyrroles: Conformationally flexible fluorometric chemosensors. *Supramol. Chem.* **2009**, *21*, 164-172.

[28] Bell, J. W.; Hext, N. M. Supramolecular optical chemosensors for organic analytes. *Chem. Soc. Rev.* **2004**, *33*, 589-598.

[29] Guinovart, T.; Hernández-Alonso, D.; Adriaenssens, L.; Blondeau, P.; Martínez-Belmonte, M.; Rius, F. X.; Andrade, F. J.; Ballester, P. Recognition and Sensing of Creatinine. *Angew. Chem., Int. Ed.* **2016**, *55*, 2435-2440.

[30] Nguyen, B. T.; Anslyn, E. V. Indicator–displacement assays. *Coord. Chem. Rev.* **2006**, *250*, 3118-3127.

[31] Nguyen, B. T.; Wiskur, S. L.; Anslyn, E. V. Using Indicator-Displacement Assays in Test Strips and To Follow Reaction Kinetics. *Org. Lett.* **2004**, *6*, 2499-2501.

[32] Escobar, L.; Aragay, G.; Ballester, P. Super Aryl-Extended Calix[4]pyrroles: Synthesis, Binding Studies, and Attempts To Gain Water Solubility. *Chem.--Eur. J.* **2016**, *22*, 13682-13689.

[33] Ciardi, M.; Tancini, F.; Gil-Ramírez, G.; Escudero Adán, E. C.; Massera, C.; Dalcanale, E.; Ballester, P. Switching from Separated to Contact Ion-Pair Binding Modes with Diastereomeric Calix[4]pyrrole Bis-phosphonate Receptors. *J. Am. Chem. Soc.* **2012**, *134*, 13121-13132.

[34] Lledó, A.; Rebek Jr, J. Self-folding cavitands: structural characterization of the induced-fit model. *Chem. Commun. (Cambridge, U. K.)* **2010**, *46*, 1637.

[35] Galán, A.; Escudero-Adán, E. C.; Frontera, A.; Ballester, P. Synthesis, Structure, and Binding Properties of Lipophilic Cavitands Based on a Calix[4]pyrrole-Resorcinarene Hybrid Scaffold. *J. Org. Chem.* **2014**, *79*, 5545-5557.

[36] Koh, K. N.; Araki, K.; Ikeda, A.; Otsuka, H.; Shinkai, S. Reinvestigation of calixarene-based artificial-signaling acetylcholine receptors useful in neutral aqueous (water/methanol) solution. *J. Am. Chem. Soc.* **1996**, *118*, 755-758.

[37] Han, F. S.; Higuchi, M.; Kurth, D. G. Diverse synthesis of novel bisterpyridines via Suzuki-type cross-coupling. *Org. Lett.* **2007**, *9*, 559-562.

[38] Pentimalli, L. Aromatic azo compounds. Oxidation of p-dimethylaminophenylazopyridines. *Tetrahedron* **1960**, *9*, 194-201.

[39] Faessinger, R. W.; Brown, E. V. Pyridine analogs of p-dimethylaminoazobenzene. *Trans. Ky. Acad. Sci.* **1963**, *24*, 106-110.

[40] Kumar, V.; Rana, H.; Kaushik, M. P. Novel and green protocol for the synthesis of 2-iminohydantoins. *Tetrahedron Lett.* **2012**, *53*, 6423-6425.

[41] Becke, A. D. Density-Functional Exchange-Energy Approximation with Correct Asymptotic-Behavior. *Phys. Rev. A* **1988**, *38*, 3098-3100.

[42] Perdew, J. P. Density-Functional Approximation for the Correlation-Energy of the Inhomogeneous Electron-Gas. *Phys Rev B* **1986**, *33*, 8822-8824.

[43] Grimme, S.; Antony, J.; Ehrlich, S.; Krieg, H. A consistent and accurate ab initio parametrization of density functional dispersion correction (DFT-D) for the 94 elements H-Pu. *J. Chem. Phys.* **2010**, *132*, 154104.

[44] Sure, R.; Brandenburg, J. G.; Grimme, S. Small Atomic Orbital Basis Set First-Principles Quantum Chemical Methods for Large Molecular and Periodic Systems: A Critical Analysis of Error Sources. *ChemistryOpen* **2016**, *5*, 94-109.

[45] Weigend, F.; Ahlrichs, R. Balanced basis sets of split valence, triple zeta valence and quadruple zeta valence quality for H to Rn: Design and assessment of accuracy. *Phys. Chem. Chem. Phys.* **2005**, *7*, 3297-3305.

[46] Gaussian 09, Revision A 02, M. J. Frisch, G. W. T., H. B. Schlegel, G. E. Scuseria, M. A. Robb, J. R. Cheeseman, G. Scalmani, V. Barone, G. A. Petersson, H. Nakatsuji, X. Li, M. Caricato, A. Marenich, J. Bloino, B. G. Janesko, R. Gomperts, B. Mennucci, H. P. Hratchian, J. V. Ortiz, A. F. Izmaylov, J. L. Sonnenberg, D. Williams-Young, F. Ding, F. Lipparini, F. Egidi, J. Goings, B. Peng, A. Petrone, T. Henderson, D. Ranasinghe, V. G. Zakrzewski, J. Gao, N. Rega, G. Zheng, W. Liang, M. Hada, M. Ehara, K. Toyota, R. Fukuda, J. Hasegawa, M. Ishida, T. Nakajima, Y. Honda, O. Kitao, H. Nakai, T. Vreven, K. Throssell, J. A. Montgomery, Jr., J. E. Peralta, F. Ogliaro, M. Bearpark, J. J. Heyd, E. Brothers, K. N. Kudin, V. N. Staroverov, T. Keith, R. Kobayashi, J. Normand, K. Raghavachari, A. Rendell, J. C. Burant, S. S. Iyengar, J. Tomasi, M. Cossi, J. M. Millam, M. Klene, C. Adamo, R. Cammi, J. W. Ochterski, R. L. Martin, K. Morokuma, O. Farkas, J. B. Foresman, and D. J. Fox, Gaussian, Inc., Wallingford CT, 2016

[47] Aksel, T.; Majumdar, A.; Barrick, D. The Contribution of Entropy, Enthalpy, and Hydrophobic Desolvation to Cooperativity in Repeat-Protein Folding**2011**, *19*, 349-360.

[48] Marras, S. A. E.; Kramer, F. R.; Tyagi, S. Efficiencies of fluorescence resonance energy transfer and contact-mediated quenching in oligonucleotide probes. *Nucleic Acids Res.* **2002**, *30*.

[49] Aggarwal, M.; Sharma, R.; Kumar, P.; Parida, M.; Tomar, S. Kinetic characterization of trans-proteolytic activity of Chikungunya virus capsid protease and development of a FRET-based HTS assay. *Sci. Rep.* **2015**, *5*.

[50] The interaction of **2** with **3** was also probed using ^{1}H NMR spectroscopy (Figure S56).

[51] The release of 0.5 equiv of **HexCr** from the **HexCr⊂2** complex to the bulk solution induced by adding 0.5 equiv of **3** was evidenced by ^{1}H NMR spectroscopy (Figure S56). The reverse experiment is not feasible to be performed at mM concentration owing to the reduced solubility of **HexCr** in chloroform solution (~ 1.5 mM).

[52] The interaction of **1** with **4** was also probed using ^{1}H NMR spectroscopy (Figure S57).

[53] The release of 0.5 equiv of **HexCr** from the **HexCr⊂1** complex to the bulk solution induced by adding 0.5 equiv of **4** was evidenced by ^{1}H NMR spectroscopy (Figure S58). The reverse experiment is not feasible to be performed at mM concentration owing to the reduced solubility of **HexCr** in chloroform solution (~ 1.5 mM).

TOC